

Quantifying and Optimizing Photocurrent via Optical Modeling of Gold Nanostar-, Nanorod-, and Dimer-decorated MoS₂ and MoTe₂

Original

Quantifying and Optimizing Photocurrent via Optical Modeling of Gold Nanostar-, Nanorod-, and Dimer-decorated MoS₂ and MoTe₂ / Cristiano, M N; Tsoulos, T V; Fabris, L. - In: THE JOURNAL OF CHEMICAL PHYSICS. - ISSN 0021-9606. - 152:1(2020), pp. 1-8. [10.1063/1.5127279]

Availability:

This version is available at: 11583/2983161 since: 2023-10-19T12:23:49Z

Publisher:

American Institute of Physics

Published

DOI:10.1063/1.5127279

Terms of use:

This article is made available under terms and conditions as specified in the corresponding bibliographic description in the repository

Publisher copyright

AIP postprint/Author's Accepted Manuscript e postprint versione editoriale/Version of Record




This article may be downloaded for personal use only. Any other use requires prior permission of the author and AIP Publishing. This article appeared in THE JOURNAL OF CHEMICAL PHYSICS, 2020, 152, 1, 1-8 and may be found at <http://dx.doi.org/10.1063/1.5127279>.

(Article begins on next page)

RESEARCH ARTICLE | JANUARY 02 2020

Quantifying and optimizing photocurrent via optical modeling of gold nanostar-, nanorod-, and dimer-decorated MoS₂ and MoTe₂ ✓

Special Collection: [Emerging Directions in Plasmonics](#)

Michele N. Cristiano  ; Ted V. Tsoulos  ; Laura Fabris 



J. Chem. Phys. 152, 014705 (2020)

<https://doi.org/10.1063/1.5127279>



CrossMark

Articles You May Be Interested In

Fabrication of nanostar arrays by nanoimprint lithography

J. Vac. Sci. Technol. B (November 2010)

Single gold nanostars enhance Raman scattering

Appl. Phys. Lett. (April 2009)

Gold nanostars reshaping and plasmon tuning mechanism

AIP Conference Proceedings (February 2013)

500 kHz or 8.5 GHz?
And all the ranges in between.

Lock-in Amplifiers for your periodic signal measurements



Find out more



Quantifying and optimizing photocurrent via optical modeling of gold nanostar-, nanorod-, and dimer-decorated MoS₂ and MoTe₂

Cite as: J. Chem. Phys. 152, 014705 (2020); doi: 10.1063/1.5127279

Submitted: 10 September 2019 • Accepted: 15 December 2019 •

Published Online: 2 January 2020



Michele N. Cristiano,¹ Ted V. Tsoulos,^{1,2,a)} and Laura Fabris¹

AFFILIATIONS

¹Department of Materials Science and Engineering, Rutgers University, 607 Taylor Road, Piscataway, New Jersey 08854, USA

²STI IGM LNET, École Polytechnique Fédérale de Lausanne, Station 9, CH-1015 Lausanne, Switzerland

Note: This paper is part of the JCP Special Topic on Emerging Directions in Plasmonics.

^{a)}theodoros.tsoulos@epfl.ch and lfabris@soe.rutgers.edu

ABSTRACT

Finite element simulations through COMSOL Multiphysics were used to optically model systems composed of Mo dichalcogenide layers (MoTe₂ and MoS₂) and Au nanoparticles (spherical dimers, nanorods, and nanostars) to understand how their fundamental material properties as well as their interactions affect the photocurrent response. The absorption cross sections of the various Au nanoparticles linearly increase with respect to their increasing dimensions, hence being ideal tunable systems for the enhancement of the electric field in the dichalcogenide layers under visible and near infrared. The photocurrent through the MoTe₂ and MoS₂ substrates was enhanced by the addition of Au nanoparticles when the plasmonic response was localized in the area of the particle in contact with the substrate. Based on these findings, the use of Au nanoparticles can greatly improve the unique photocurrent properties of Mo dichalcogenides; however, nanoparticle orientation and size must be considered to tune the enhancement at the specific wavelengths. This computational work provides useful design rules for the use of plasmonic nanomaterials in photocatalytic and photocurrent enhancement of transition metal dichalcogenides.

Published under license by AIP Publishing. <https://doi.org/10.1063/1.5127279>

INTRODUCTION

Two-dimensional materials have been attracting increasing interest for possible applications in catalysis,¹ sensing,² and energy storage.³ In particular, transition metal dichalcogenides (TMDs) are emerging within this class of materials. These materials have the structure MX₂, where M is a transition metal and X is a chalcogen.⁴ Their structure contains layers held together by weak van der Waals forces, allowing the material to be exfoliated from its bulk state of many layers down to a monolayer thickness.⁵ As the semiconductor changes from bulk to a monolayer, the bandgap transitions from indirect to direct bandgap, accompanied as well by a modification of the valence and conduction band edges.⁴ This crossover⁶ in the bandgap brings about unique optical and photocatalytic properties.⁷

Gold nanostructures have also emerged as promising materials for plasmonic applications in catalysis,⁸ photovoltaics,⁹ hot electron-based devices,¹⁰ and biomedicine.^{11,12} Through their surface plasmon resonances, these nanomaterials can serve as electric field enhancers or broad-band absorbers.¹³ Plasmonic materials enhance the electric field at resonant frequencies, whose position is influenced by the morphology of the nanoparticle, its orientation with respect to the polarization of the impinging radiation, and the dielectric properties of the surrounding environment.¹⁴

Combining the unique properties of both TMDs and plasmonic nanoparticles has led to important technical innovations in the areas of solar cells,¹⁵ optoelectronics,^{16–18} and electrocatalysis.¹⁹ Understanding the behavior of TMDs and nanoparticle systems especially in the case of monolayers is not trivial. Theoretically, it requires combined density functional theory for the TMDs^{20,21} and

quantum plasmonic studies for the nanoparticles²² or both.²³ Contrary to other monolayer materials, however, that require a whole different modeling approach,^{24,25} the optical absorption properties of TMDs can be quantified by classical electrodynamics. As we will show later, our approach can successfully predict even the maximized absorption of the system as we move from multilayer-level thicknesses to monolayers.

Motivated by our ability to predict the optical behavior of the two most common forms of TMDs, namely, MoS₂ and MoTe₂, we investigate in this work their optical and photocurrent properties when decorated by plasmonic nanoparticles. Our hypothesis stems from the unique electric field enhancement properties of the plasmonic nanomaterials and their coupling mechanisms,^{26–31} and the need for quantification and optimization of the complex resulting TMD-nanoparticle systems. We propose that the photocurrent properties through monolayered and multilayered systems can be effectively improved when the plasmonic nanomaterials are in direct contact with the TMDs by greatly enhancing the electric field in the nanoparticle vicinity and therefore the current density in the TMDs. By using finite element simulations, we have explored the optical and photocurrent properties of three gold nanoparticle shapes on two different TMD substrates. Ultimately, optimal design rules for these gold plasmonic nanomaterials are proposed to enhance the photocurrent properties of MoS₂ and MoTe₂.

Our optimization method is built on three main steps, executed in the following order: (1) We secure optimal resonant conditions of standalone particles with respect to maximum absorption by tuning the size and polarization alignment with the incoming field. (2) We optimize the distance between the particle and the substrate with respect to maximum photocurrent (as seen in the [supplementary material](#) for the nanorod case). (3) Most importantly, and the basis of this work, we search for the optimal resonant feature alignment between the particles and the TMDs to maximize photocurrent. Interestingly, and contrary to common practice, the optimal case does not originate when the impinging radiation is in resonance with the particle's plasmonic modes, rather it is realized when hybrid modes between the particles and the substrate localize the maximum field enhancement onto the substrate. In other words, the maximum photocurrent is reported when the Au nanoparticle-TMD systems resonate next to or in contact with the substrate.

METHODS

For understanding the structure–property relationship between gold nanoparticles and transition metal dichalcogenides and their effect on optical and photocatalytic properties, we designed models of each individual component and of the combinations of the components, i.e., the standalone substrate *in vacuo*, the gold nanoparticle in water, and the gold nanoparticle on the substrate *in vacuo*. The RF module of COMSOL Multiphysics 5.3 was used to simulate the optical and photocurrent behavior of the various systems with linearly polarized light defined by Eq. (1), while the absorption and optical properties were calculated according to our previously published works.^{13,32–34} In addition to what we have previously shown, we calculate the photocurrent according to Eq. (2), by integrating

the current density J over a plane cut perpendicular to the surface of the TMDs,

$$E = E_0 e^{jk_0 z} \hat{x}. \quad (1)$$

In all of the simulations presented in this work, we define an arbitrary electric field amplitude of $E_0 = 1014.889$ V/m to reflect the magnitude of the average intensity of the solar energy on earth, as a figure of merit for potential applications of the various systems studied. To minimize the edge scattering effects of the geometry, we extended the substrate into the perfectly matched layer (PML). As seen in Eq. (2), the photoinduced current was calculated by integrating J over a lateral cut in the substrate. To understand the phenomenon in a 3D space, we average the photocurrent obtained between two planes—one parallel to the direction of the incoming light polarization ($x = 0$ plane) and one perpendicular to this direction ($y = 0$ plane)—as follows: $I_{AVG} = \frac{1}{2} \iint J dx dz + \frac{1}{2} \iint J dy dz$, i.e.,

$$I = \iint J dx dz = \iint \sigma E dx dz. \quad (2)$$

The absorption cross section was used to examine the optical properties of the nanoparticle, TMD system, as this corresponds to a measured experimental absorbance spectrum. This parameter was normalized according to volume, i.e., the normalized absorption cross section of the nanoparticle according to the nanoparticle volume and the normalized absorption cross section of the substrate according to the 2D material layer volume. We focus on the absorption of both TMDs and nanoparticles as the absorbed energy is the one contributing to the resistive losses and thus the generated photocurrent. The local scattered field of the particle and the field enhancement hot spots contribute to the generated photocurrent in the TMD substrate as part of the local E/M interaction between the two systems; this is taken into account as we solve for the scattered field first and then integrate for the losses and the current flow.

Transition metal dichalcogenides 2H-MoS₂ and 2H-MoTe₂ were modeled as standalone systems with varying thicknesses to observe their contribution to the optical response. Monolayer thicknesses of MoS₂ and MoTe₂ are 6.5 Å³⁵ and 6.97 Å,³⁶ respectively. As the material changes from its bulk state to the monolayer, an indirect to direct bandgap crossover occurs due to the confinement of electrons within the material. Standalone Au spherical dimers, Au nanorods, and Au nanostars were modeled with different sizes to evaluate their optical properties. Among all possible nanostar morphologies, we chose our recently demonstrated six-branched nanostars due to their narrower and more intense localized surface plasmon resonance (LSPR) bands.^{13,34} Each nanostructure was then modeled while in contact with the surface of the TMD to investigate the impact of this coupling on the optical and photocatalytic response. The TMD-nanoparticle systems were all modeled with a TMD thickness of 10 nm as this provided a good platform for comparison of easily synthesized few-layered TMDs and nanoparticles of comparable sizes. The TMDs at 10 nm, while multilayered, still exhibit the effects of the bandgap transition and the resulting desirable properties. [Figure 1](#) displays the standalone geometries of each of the constituent part models. Material properties were defined

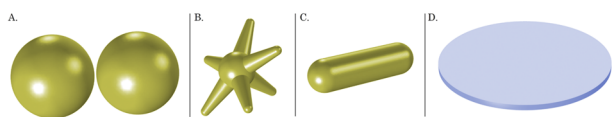


FIG. 1. Geometries created for optical modeling of plasmonic (a) spherical dimers, (b) nanostars, (c) nanorods, and (d) 2D transition metal dichalcogenides.

using the frequency-dependent dielectric functions $\epsilon(f)$ from Beal and Hughes³⁷ for the TMDs and from Johnson and Christy³⁸ for the Au nanoparticles.

RESULTS AND DISCUSSION

In this study, we investigate the fundamental material properties of Mo dichalcogenides and Au nanoparticles as well as the interactions between these materials. In particular, we develop engineering design requirements through the computational method presented above to improve the optical and photocatalytic properties of 2D transition metal dichalcogenides by using plasmonic nanoparticles.

Standalone Mo dichalcogenides

Using optical modeling, various thicknesses of MoS₂ and MoTe₂ substrates were investigated to understand the difference in optical properties of the bulk and monolayer material. Figure 2(a) displays the absorption cross section of MoS₂, normalized according to the volume of the substrate. The absorption profile of MoS₂ layers of variable thickness, calculated with our method, adequately matched the measured experimental absorbance of MoS₂ from the work of Wang *et al.*³⁹ The agreement between peak positions, and importantly, relative intensities, validates our method in predicting the experimental optical properties of MoS₂. Figure 2(a) also shows an increase in the normalized absorption cross section as the substrate thins to the limit of a monolayer. This corresponds to the transition from an indirect to direct bandgap material, which gives

rise to the unique optical properties of transition metal dichalcogenide monolayers. Figure 2(b) displays the normalized absorption cross section of MoTe₂. The spectrum for this TMD also adequately matches experimental absorbance as determined by Heinz and co-workers.⁴⁰

Standalone Au nanoparticles

Au spherical dimers, nanorods, and nanostars were modeled individually in water^{13,32} with various sizes. A strong positive linear relationship between the peak wavelength of absorption cross section and the nanoparticle size [that is dimers of spheres with 50, 60, 70, and 80 nm diameter; nanostars with 60, 80, and 100 nm spike length (Fig. S1); and nanorods with 35, 45, 55 nm length, and 15 nm constant thickness] was determined for all morphologies modeled, providing useful information for a tunable system that enhances the electric field as light is shone. Figure 3 displays the relations found for the nanoparticles. The relative intensities of the normalized absorption cross section peaks should be noted as they correspond to the amount of enhancement of the surrounding electric field. Particle orientation with respect to the incoming field polarization was also found to be important for the absorption spectrum, as previously shown in the literature.⁴¹ As a result of several optimization studies (Fig. S2), the Au spherical dimers were kept at 2 nm separation, and the interparticle axis was kept parallel to the polarization of the impinging light. The Au nanorods were aligned at 60° with the incoming field polarization (Fig. S3) in order to represent both the longitudinal and the transverse modes. The Au nanostars were kept at 51° with respect to the surface of the TMD to maximize the current enhancement and to provide a realistic placement with three spikes being in contact with the TMD. The Au nanostars were also placed so that two spikes were aligned parallel with the incoming light polarization axis, and a third spike was touching along the yz-plane. The orientation configurations of the dimers, nanorods, and nanostars were optimized and determined based on maximum absorption so as to secure maximum photocurrent from the particles-TMDs systems. For the standalone particle cases, we first optimized the orientations and the aspect ratios that yielded maximum absorption in the visible and

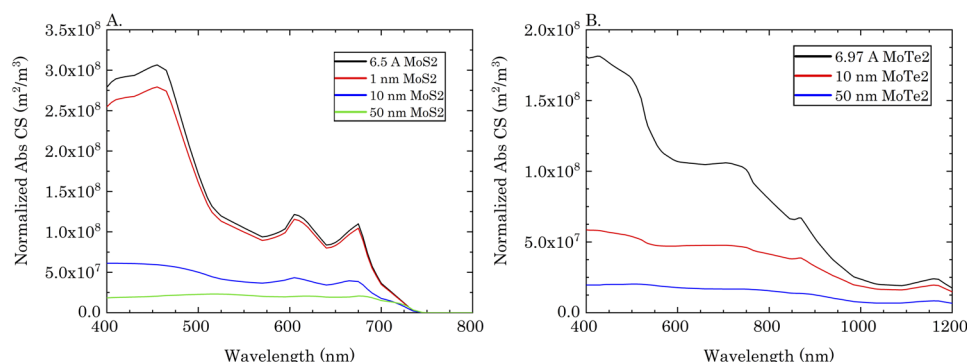


FIG. 2. From single layer thickness to 50 nm, we plot the normalized absorption cross section for (a) MoS₂ and (b) MoTe₂. The values were determined through optical modeling. As the layer thickness decreases, the normalized absorption cross section increases, with relative intensities for monolayer thicknesses matching those experimentally determined in the literature. Unlike other thin and 2D materials, MoS₂ and MoTe₂ can be optically modeled with classic electromagnetic numerics down to the monolayer.

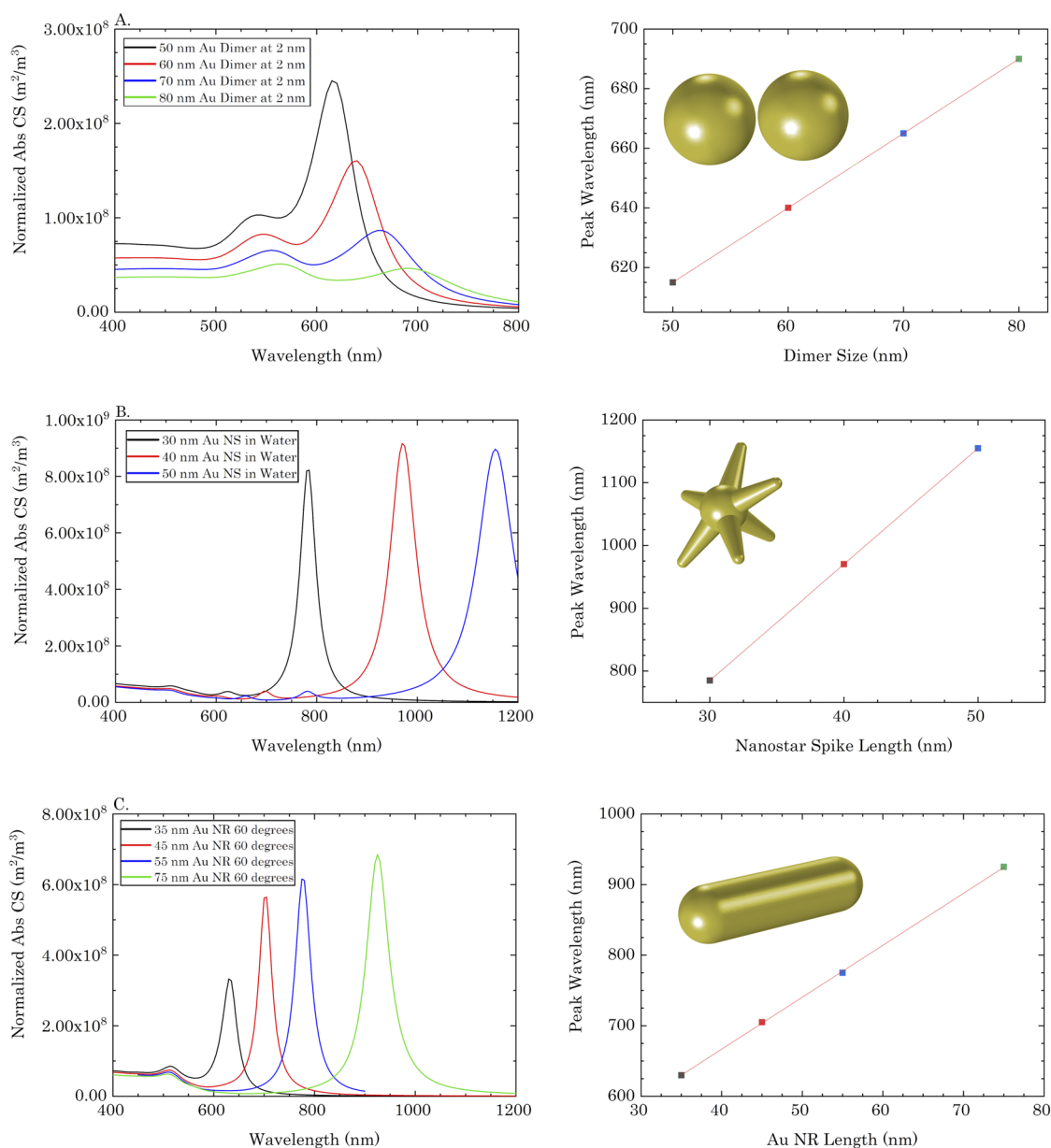


FIG. 3. Optimized aspect ratios and orientations of gold dimers, nanorods, and nanostars in the visible-NIR region with respect to maximum absorption and their size dependence. This optimization leads to maximum particle absorption which then provides maximum photocurrent for the particle-TMD systems. (a) Au spherical dimers decrease in σ_{Abs} for both the longitudinal and transverse peaks with increasing diameter. (b) As expected σ_{Abs} of Au nanostars red-shifts with increasing spike length. (c) Increasing the lengths of Au nanorods with a constant diameter of 15 nm red-shifts the longitudinal peak and increases its intensity. All particles were determined to have a strong positive linear correlation between their size and the wavelength of the peak longitudinal absorption cross section.

near-infrared (NIR) regions and then we varied the size as presented in Fig. 3.

Au nanoparticles on Mo dichalcogenides

Three sizes of Au spherical dimers and nanostars are modeled on both MoS_2 and MoTe_2 , along with three sizes of Au

nanorods on MoTe_2 . The absorption cross sections of each component of the systems are calculated and normalized with respect to particle volume. The current through the 2D transition metal dichalcogenides is also calculated and compared to the standalone models. Figures 4–6 show the changes in absorption cross section and current with various plasmonic nanostructure sizes. The Au nanostars exhibit greater enhancement compared to the Au

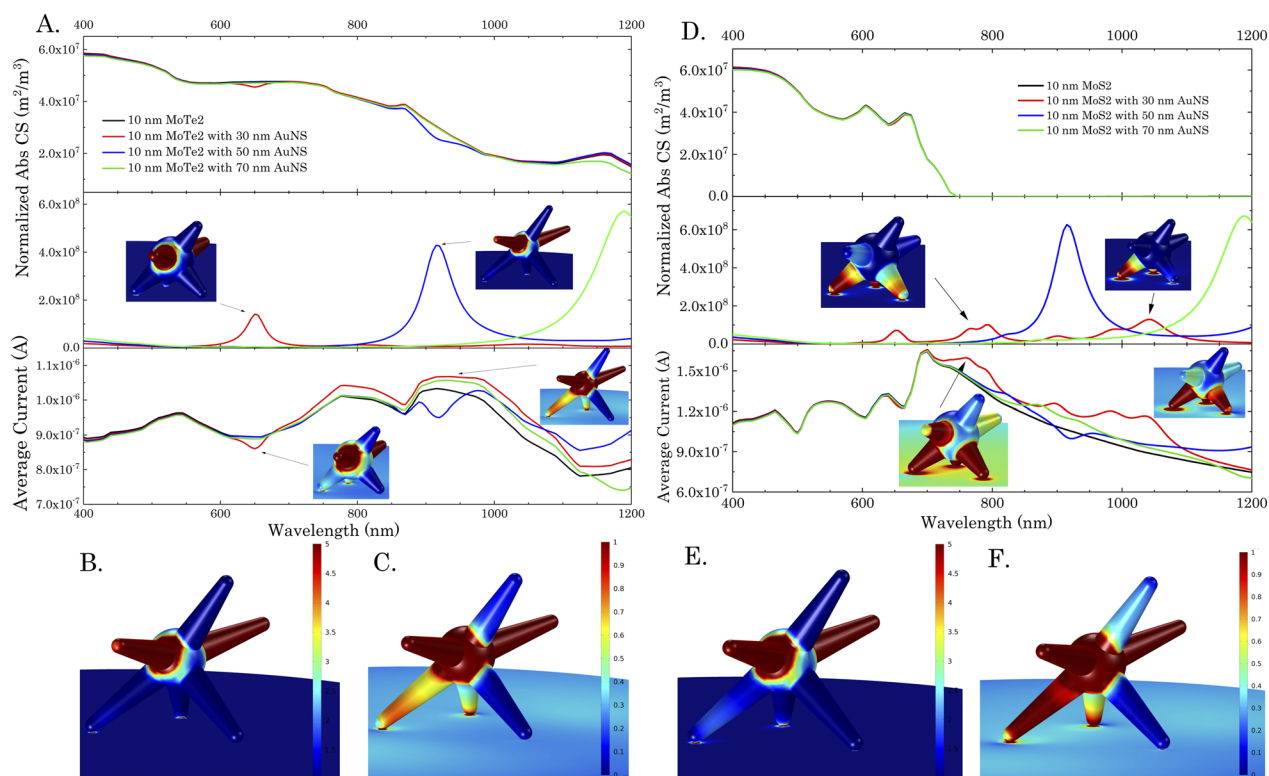


FIG. 4. Gold nanostars enhance significantly the photocurrent of both MoTe₂ and MoS₂ from 750 to 1200 nm with the enhancement in MoTe₂ being more broadband and in MoS₂ being interestingly tailored to the nanostar resonant profile. The latter could be exploited for targeted narrowband applications. (a) Au nanostars on MoTe₂ cause a broadband increase in the photocurrent when the nanostar spikes in contact with the MoTe₂ resonate, and they cause a decrease when the spikes not in contact resonate. (b) At 925 nm, for a 50 nm Au nanostar, the spikes not in contact with MoTe₂ resonate and (c) the photocurrent is limited in the substrate. (d) Narrowband increase in the photocurrent in the case of nanostars on a MoS₂ layer. (e) At 995 nm, a 30 nm Au nanostar exhibits an at least 5-fold enhancement of the electric field on the spikes in contact with the substrate and (f) the current density through MoS₂ at least doubles within a 45 nm band.

spherical dimers due to the greater electric field enhancement of the nanostars at the points of contact with the TMD substrate. When the nanoparticle displays a plasmonic behavior, a hot spot is created where the enhanced electric field is maximized. For the Au nanostars, this enhancement occurs on the spike tips; however, different resonant wavelengths correspond to different spikes being enhanced. When the spikes that are not in contact with the TMD substrate resonate and exhibit hot spots, the current density is shown to decrease the current through the substrate at that particular wavelength. On the contrary, when the nanostar spikes that are in contact with the TMD substrate resonate and exhibit hot spots, the current through the substrate is significantly increased. This stands as a strong argument for the use of plasmonic nanoparticles for enhancing the unique photocatalytic properties of TMDs if the correct morphology and orientation are taken into consideration.

To assess the validity of this statement, we explored numerous configurations and combinations of spike alignment with respect to the incoming field polarization while varying also how the spikes contact the substrate and how many of them are in touch with the TMD. In all cases, the maximum photocurrent is achieved

when the maximum number of spikes aligns with the field polarization and with each other while staying in touch with the substrate (considering stars with more spikes as well¹³). Most importantly, (1) the number of spikes touching the substrate should exceed two as this condition favors channeling the exiting current, and (2) the spikes should be inserted in the direction of the field polarization.

Au nanorods display a similar behavior. The enhancement of the electric field along the TMD oscillates at the tips of the Au nanorod at its plasmonic frequency, which corresponds to an enhanced photocurrent through the TMD for those frequencies. At the characteristic wavelengths of enhancement, the current density flows through the nanorod, redirecting the line of current, as the rod was placed at 60° with respect to the direction of polarization, according to the optimization rules described above for maximum absorption and current. We also explored embedding the nanorods in the substrate (as shown in Fig. S4 of the [supplementary material](#)). This study yielded the conclusion that the optimal case is to allow a slight embedding as they both resonate the strongest and provide current flow to and from the substrate. These results may relate to the other nanoparticle geometries as well.

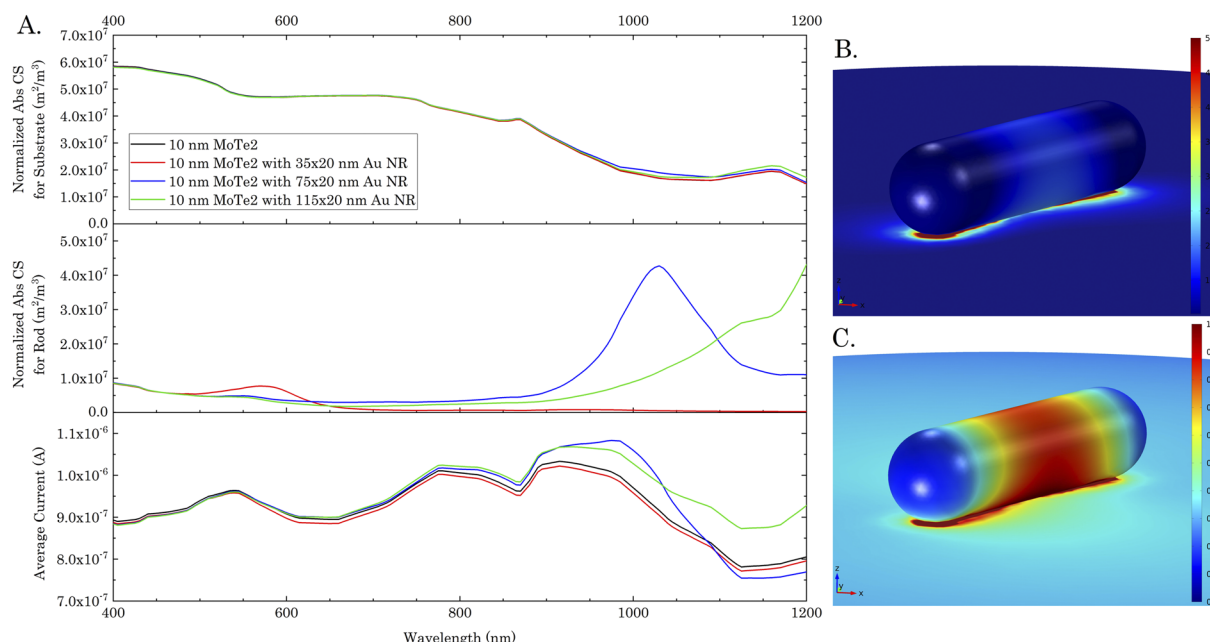


FIG. 5. Au nanorods enhance the photocurrent in a MoTe₂ substrate in a broadband manner following the absorptive profile of the particles. (a) Different aspect ratios were optically modeled in contact with MoTe₂. (b) At 1030 nm, a 75 × 20 nm Au nanorod enhances the electric field along its tips on the substrate causing a (c) current flow increase through MoTe₂ at the resonant hot spots of the system.

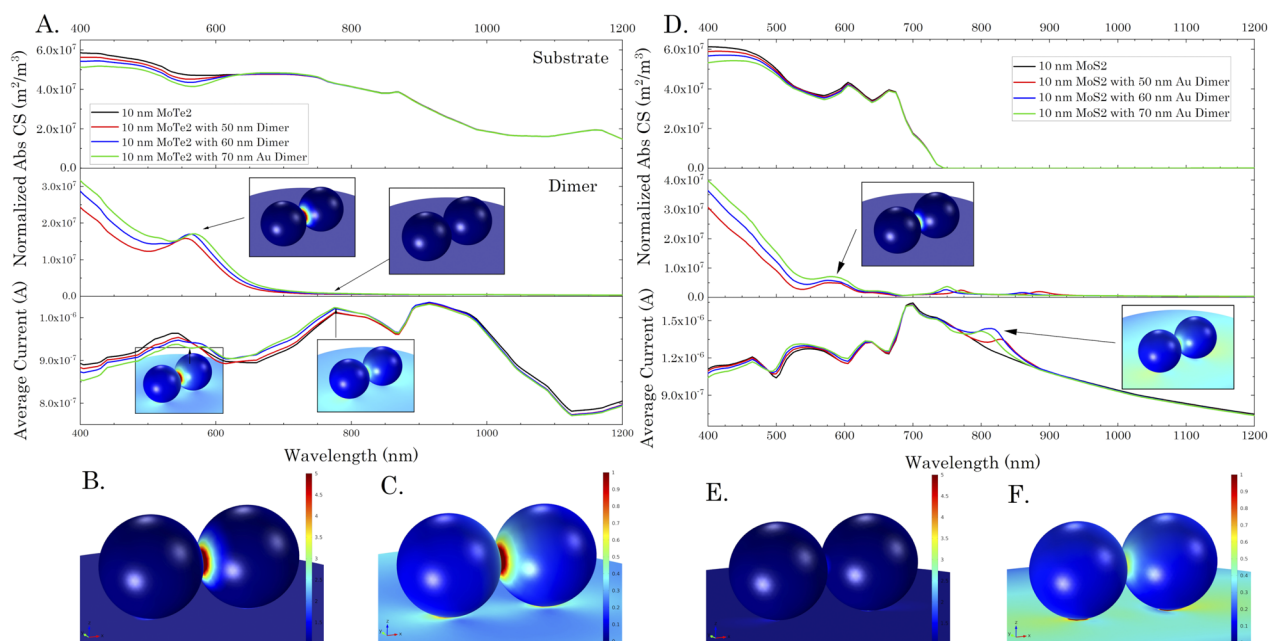


FIG. 6. (a) MoTe₂ with various sizes of Au spherical dimers display a slight increase in current when the normalized absorption cross section of the dimer experiences an enhancement on the bottom of the spheres in contact with the TMD and a decrease in current when the enhancement is in the junction. (b) At 570 nm, the 70 nm Au dimer resonates between the spheres, and the electric field is denser in those regions. (c) The current density of the 70 nm Au nanostar at 565 nm on MoTe₂ forms cells between the enhanced spheres, limiting the current flowing through the substrate. (d) Similar material design rules were displayed for the Au spherical dimers on a MoS₂ layer. (e) At 750 nm, the 60 nm Au dimer was enhanced on the part of the spheres in contact with the TMD. (f) The current density through MoS₂ was enhanced at 815 nm by flowing through the enhanced field region in contact with the substrate.

Nanorods also show a broader range of enhancement compared to nanostars when in contact with TMDs, making them possibly more beneficial for applications where a larger range of frequencies needs to be enhanced, while nanostars may be better suited for targeted applications and maximum photocurrent. However, the experimental constraints to be met to achieve this specific nanostar orientation on the TMDs so that such photocurrent is obtained should be always considered. In brief, both nanostars and nanorods enhance the photocurrent significantly from 900 to 1200 nm and even a simple drop-casting deposition should yield measurable increases.

Limited improvement in photocurrent properties is achieved by using spherical dimers as the majority of the resonance is localized between the spheres rather than at the point of contact with the substrate. Although dimers do provide a measurable increase in the photocurrent of the TMDs, Au nanorods and nanostars are more tunable and they are therefore a better fit for the purpose of this project. Nevertheless, it would be interesting to see the collective behavior of several dimer groups on TMDs with a strong computational unit or with an experimental design as both dimers and TMDs are rather well studied and relatively easy to combine. Larger sizes of Au nanorods and nanostars resonate in red-shifted spectral positions as it is well known,^{42,43} and as a result, they do redshift the wavelength of the maximum current enhancement in the TMD.

Plasmonic nanoparticles that are too long possess resonances that are red-shifted too far in the spectrum to provide notable enhancement in the optical and biological windows, i.e., from 400 to 1200 nm. Nanoparticles that are too small, on the other hand, do not provide enough electric field enhancement to effectively increase the current through the transition metal dichalcogenide. When designing a system with plasmonic nanoparticles and transition metal dichalcogenides, optimization in morphology and orientation is crucial to obtain significant photocatalytic property improvements at a desired wavelength.

CONCLUSIONS

Gold nanoparticles effectively enhance the optical and photocurrent properties of molybdenum dichalcogenides. As we present, optimizing and quantifying this enhancement is crucial and should be based on (1) nanoparticle shape and type, (2) points of physical contact, (3) light polarization, and (4) relative particle orientation. Based on our three-step optimization method, the optimal distance between nanoparticle and TMD substrate for photocurrent maximization is ~ 5 nm, i.e., the particle should get partially embedded in the TMD if chemically possible. Contrary to what previously suggested, simply aiming to achieve resonance with the nanoparticle modes does not lead to the ideal case, even if one takes into account the TMD substrate. Rather, it is necessary to consider that each TMD-nanoparticle system exhibits distinguishable TMD-particle hybrid states that localize the field enhancement at the particle-TMD interface. These hybrid resonances are those that should be modeled and targeted in order to maximize photocurrent. Although gold nanostars provide the maximum photocurrent enhancement, gold nanorods are possibly best suited to achieve photocurrent maximization owing to more straightforward establishment of contact

with the substrate and the tunability of their plasmonic modes. Gold nanosphere dimers do not compete with either even though a collective effect may be expected to multiply the individual contributions as the hot spots of the hybrid modes lead to some enhancement. We conclude on the crucial importance of the engineering design rules for using plasmonic nanoparticles to enhance the photocurrent (for photocatalysis, solar cells, and sensing) properties of multi-layer transition metal dichalcogenides. We propose a simple optical modeling method that is achievable for this design with limited computational power and resources (a laptop was used for the current work). This method could be ideally suited, for instance, to guide in real time the synthesis and development of TMD—nanoparticle systems.

SUPPLEMENTARY MATERIAL

See the [supplementary material](#) for schematic with details on nanostar morphology and optimization of nanoparticle separation in dimers, nanorod orientation, and nanorod interaction with a substrate.

REFERENCES

- ¹D. Deng, K. S. Novoselov, Q. Fu, N. Zheng, Z. Tian, and X. Bao, "Catalysis with two-dimensional materials and their heterostructures," *Nat. Nanotechnol.* **11**, 218 (2016).
- ²H. Morgan, C. S. Rout, and D. J. Late, "Future prospects of 2D materials for sensing applications," in *Fundamentals and Sensing Applications of 2D Materials*, edited by M. Hywel, C. S. Rout, and D. J. Late (Woodhead Publishing, 2019), Chap. 14, pp. 481–482.
- ³R. Mas-Balleste, C. Gomez-Navarro, J. Gomez-Herrero, and F. J. N. Zamora, "2D materials: To graphene and beyond," *Nanoscale* **3**, 20–30 (2011).
- ⁴S. Manzeli, D. Ovchinnikov, D. Pasquier, O. V. Yazyev, and A. Kis, "2D transition metal dichalcogenides," *Nat. Rev. Mater.* **2**, 17033 (2017).
- ⁵H. Tian, M. L. Chin, S. Najmaei, Q. Guo, F. Xia, H. Wang, and M. Dubey, "Optoelectronic devices based on two-dimensional transition metal dichalcogenides," *Nano Res.* **9**, 1543–1560 (2016).
- ⁶L. Ortenzi, L. Pietronero, and E. Cappelluti, "Zero-point motion and direct-indirect band-gap crossover in layered transition-metal dichalcogenides," *Phys. Rev. B* **98**, 195313 (2018).
- ⁷R. Lv, J. A. Robinson, R. E. Schaak, D. Sun, Y. Sun, T. E. Mallouk, and M. Terrones, "Transition metal dichalcogenides and beyond: Synthesis, properties, and applications of single- and few-layer nanosheets," *Acc. Chem. Res.* **48**, 56–64 (2015).
- ⁸C. Qianling, B. Xia, S. Mitzscherling, A. Masic, L. Li, M. Bargheer, and H. Moehwald, "Preparation of gold nanostars and their study in selective catalytic reactions," *Colloids Surf., A* **465**, 20 (2015).
- ⁹H. Elbohy, M. R. Kim, A. Dubey, K. M. Reza, D. Ma, J. Zai, X. Qian, and Q. Qiao, "Incorporation of plasmonic Au nanostars into photoanodes for high efficiency dye-sensitized solar cells," *J. Mater. Chem. A* **4**, 545–551 (2016).
- ¹⁰A. Sousa-Castillo, M. Comesaña-Hermo, B. Rodríguez-González, M. Pérez-Lorenzo, Z. Wang, X.-T. Kong, A. O. Govorov, and M. A. Correa-Duarte, "Boosting hot electron-driven photocatalysis through anisotropic plasmonic nanoparticles with hot spots in Au-TiO₂ nanoarchitectures," *J. Phys. Chem. C* **120**, 11690–11699 (2016).
- ¹¹Y. Liu, H. Yuan, A. M. Fales, J. K. Register, and T. Vo-Dinh, "Multifunctional gold nanostars for molecular imaging and cancer therapy," *Front. Chem.* **3**, 51 (2015).
- ¹²Y. I. Park, H. Im, R. Weissleder, and H. Lee, "Nanostar clustering improves the sensitivity of plasmonic assays," *Bioconjugate Chem.* **26**, 1470–1474 (2015).
- ¹³T. V. Tsoulos and L. Fabris, "Interface and bulk standing waves drive the coupling of plasmonic nanostar antennas," *J. Phys. Chem. C* **122**, 28949–28957 (2018).

- ¹⁴J. Langer, S. M. Novikov, and L. M. Liz-Marzán, "Sensing using plasmonic nanostructures and nanoparticles," *Nanotechnology* **26**, 322001 (2015).
- ¹⁵X. Yang, W. Liu, M. Xiong, Y. Zhang, T. Liang, J. Yang, M. Xu, J. Ye, and H. Chen, "Au nanoparticles on ultrathin MoS₂ sheets for plasmonic organic solar cells," *J. Mater. Chem. A* **2**, 14798–14806 (2014).
- ¹⁶D. Qi, Q. Wang, C. Han, J. Jiang, Y. Zheng, W. Chen, W. Zhang, and A. T. S. Wee, "Reducing the Schottky barrier between few-layer MoTe₂ and gold," *2D Mater.* **4**, 045016 (2017).
- ¹⁷J. Miao, W. Hu, Y. Jing, W. Luo, L. Liao, A. Pan, S. Wu, J. Cheng, X. Chen, and W. Lu, "Surface plasmon-enhanced photodetection in few layer MoS₂ phototransistors with Au nanostructure arrays," *Small* **11**, 2392–2398 (2015).
- ¹⁸Z. Ni *et al.*, "Plasmonic silicon quantum dots enabled high-sensitivity ultra-broadband photodetection of graphene-based hybrid phototransistors," *ACS Nano* **11**, 9854–9862 (2017).
- ¹⁹J. Kim, S. Byun, A. J. Smith, J. Yu, and J. Huang, "Enhanced electrocatalytic properties of transition-metal dichalcogenides sheets by spontaneous gold nanoparticle decoration," *J. Phys. Chem. Lett.* **4**, 1227–1232 (2013).
- ²⁰M. Javaid, D. W. Drumm, S. P. Russo, and A. D. Greentree, "A study of size-dependent properties of MoS₂ monolayer nanoflakes using density-functional theory," *Sci. Rep.* **7**, 9775 (2017).
- ²¹W. Huang, X. Luo, C. K. Gan, S. Y. Quek, and G. Liang, "Theoretical study of thermoelectric properties of few-layer MoS₂ and WSe₂," *Phys. Chem. Chem. Phys.* **16**, 10866–10874 (2014).
- ²²M. S. Tame, K. R. McEnery, Ş. K. Özdemir, J. Lee, S. A. Maier, and M. S. Kim, "Quantum plasmonics," *Nat. Phys.* **9**, 329 (2013).
- ²³Y. Li, Z. Li, C. Chi, H. Shan, L. Zheng, and Z. Fang, "Plasmonics of 2D nanomaterials: Properties and applications," *Adv. Sci.* **4**, 1600430 (2017).
- ²⁴N. K. Emani, T.-F. Chung, X. Ni, A. V. Kildishev, Y. P. Chen, and A. Boltasseva, "Electrically tunable damping of plasmonic resonances with graphene," *Nano Lett.* **12**, 5202–5206 (2012).
- ²⁵N. K. Emani, T.-F. Chung, A. V. Kildishev, V. M. Shalae, Y. P. Chen, and A. Boltasseva, "Electrical modulation of fano resonance in plasmonic nanostructures using graphene," *Nano Lett.* **14**, 78–82 (2014).
- ²⁶J. Wu *et al.*, "Two-dimensional molybdenum disulfide (MoS₂) with gold nanoparticles for biosensing of explosives by optical spectroscopy," *Sens. Actuators, B* **261**, 279–287 (2018).
- ²⁷S. Su, M. Zou, H. Zhao, C. Yuan, Y. Xu, C. Zhang, L. Wang, C. Fan, and L. Wang, "Shape-controlled gold nanoparticles supported on MoS₂ nanosheets: Synergistic effect of thionine and MoS₂ and their application for electrochemical label-free immunosensing," *Nanoscale* **7**, 19129–19135 (2015).
- ²⁸N. Fu, Y. Hu, S. Shi, S. Ren, W. Liu, S. Su, B. Zhao, L. Weng, and L. Wang, "Au nanoparticles on two-dimensional MoS₂ nanosheets as a photoanode for efficient photoelectrochemical miRNA detection," *Analyst* **143**, 1705–1712 (2018).
- ²⁹P. Zuo *et al.*, "Shape-controllable gold nanoparticle–MoS₂ hybrids prepared by tuning edge-active sites and surface structures of MoS₂ via temporally shaped femtosecond pulses," *ACS Appl. Mater. Interfaces* **9**, 7447–7455 (2017).
- ³⁰S. Diefenbach *et al.*, "Manifold coupling mechanisms of transition metal dichalcogenides to plasmonic gold nanoparticle arrays," *J. Phys. Chem. C* **122**, 9663–9670 (2018).
- ³¹W. Liu, B. Lee, C. H. Naylor, H.-S. Ee, J. Park, A. T. C. Johnson, and R. Agarwal, "Strong exciton–plasmon coupling in MoS₂ coupled with plasmonic lattice," *Nano Lett.* **16**, 1262–1269 (2016).
- ³²S. Atta, T. V. Tsoulos, and L. Fabris, "Shaping gold nanostar electric fields for surface-enhanced Raman spectroscopy enhancement via silica coating and selective etching," *J. Phys. Chem. C* **120**, 20749–20758 (2016).
- ³³T. V. Tsoulos, L. Han, J. Weir, H. L. Xin, and L. Fabris, "A closer look at the physical and optical properties of gold nanostars: An experimental and computational study," *Nanoscale* **9**, 3766–3773 (2017).
- ³⁴T. V. Tsoulos, S. Atta, M. J. Lagos, M. Beetz, P. E. Batson, G. Tsilomelekis, and L. Fabris, "Colloidal plasmonic nanostar antennas with wide range resonance tunability," *Nanoscale* **11**, 18662–18671 (2019).
- ³⁵B. Radisavljevic, A. Radenovic, J. Brivio, V. Giacometti, and A. Kis, "Single-layer MoS₂ transistors," *Nat. Nanotechnol.* **6**, 147 (2011).
- ³⁶R. F. Frindt, "The optical properties of single crystals of WSe₂ and MoTe₂," *J. Phys. Chem. Solids* **24**, 1107–1108 (1963).
- ³⁷A. R. Beal and H. P. Hughes, "Kramers-Kronig analysis of the reflectivity spectra of 2H-MoS₂, 2H-MoSe₂ and 2H-MoTe₂," *J. Phys. C: Solid State Phys.* **12**, 881–890 (1979).
- ³⁸P. B. Johnson and R. W. Christy, "Optical constants of the noble metals," *Phys. Rev. B* **6**, 4370–4379 (1972).
- ³⁹K. Wang *et al.*, "Ultrafast saturable absorption of two-dimensional MoS₂ nanosheets," *ACS Nano* **7**, 9260–9267 (2013).
- ⁴⁰C. Ruppert, O. B. Aslan, and T. F. Heinz, "Optical properties and band gap of single- and few-layer MoTe₂ crystals," *Nano Lett.* **14**, 6231–6236 (2014).
- ⁴¹W.-S. Chang, J. W. Ha, L. S. Slaughter, and S. Link, "Plasmonic nanorod absorbers as orientation sensors," *Proc. Natl. Acad. Sci. U. S. A.* **107**, 2781–2786 (2010).
- ⁴²E. K. Payne, K. L. Shuford, S. Park, G. C. Schatz, and C. A. Mirkin, "Multipole plasmon resonances in gold nanorods," *J. Phys. Chem. B* **110**, 2150–2154 (2006).
- ⁴³F. Hao, C. L. Nehl, J. H. Hafner, and P. Nordlander, "Plasmon resonances of a gold nanostar," *Nano Lett.* **7**, 729–732 (2007).